

II. Voltage-activated Proton Currents in Human THP-1 Monocytes

T.E. DeCoursey, V.V. Cherny

Department of Molecular Biophysics and Physiology, Rush Presbyterian St. Luke's Medical Center, 1653 West Congress Parkway, Chicago, IL 60612

Received: 19 September 1995/Revised: 14 March 1996

Abstract. Depolarization-activated H^+ -selective currents were studied using whole-cell and excised-patch voltage clamp methods in human monocytic leukemia THP-1 cells, before and after being induced by phorbol ester to differentiate into macrophage-like cells. The H^+ conductance, g_H , activated slowly during depolarizing pulses, with a sigmoidal time course. Fitted by a single exponential following a delay, the activation time constant, τ_{act} was roughly 10 sec at threshold potentials, decreasing at more positive potentials. Tail currents upon repolarization decayed mono-exponentially at all potentials. The tail current time constant, τ_{tail} , was voltage dependent, decreasing with hyperpolarization from 2–3 sec at 0 mV to ~200 msec at -100 mV. Surprisingly, although τ_{act} depended strongly on pH_o , τ_{tail} was completely independent of pH_o . H^+ currents were inhibited by Zn^{2+} . Increasing pH_o or decreasing pH_i shifted the voltage-activation relationship to more negative potentials, tending to activate the g_H at any given voltage. Studied in excised, inside-out membrane patches, H^+ currents were larger and activated much more rapidly at lower bath pH (i.e., pH_i). In THP-1 cells differentiated into macrophages, the H^+ current density was reduced by one-half, and τ_{act} was slower by about twofold. The properties of H^+ channels in THP-1 cells and in other macrophage-related cells are compared.

Key words: THP-1 — Proton channels — Macrophage — Phagocytes — Monocyte — pH

Introduction

The THP-1 human monocytic leukemia cell line is a useful model of cellular regulation and differentiation in the

monocytic lineage (Auwerx, 1991). In the previous paper we characterized several types of ion channels in THP-1 cells (Kim, Silver & DeCoursey, 1996). Here we describe the properties of voltage-activated H^+ -selective currents in these cells. H^+ currents have been reported in a number of cells, including a variety of phagocytes, and appear to be designed to extrude acid equivalents from cells (DeCoursey & Cherny, 1994a). The H^+ conductance, g_H , of human neutrophils has been shown to increase during the respiratory burst, where it may compensate for H^+ produced by NADPH oxidase (Henderson, Chappell & Jones, 1987, 1988a, 1988b). The net result of activation of NADPH oxidase is the release of O_2^- into the phagocytic vacuole and H^+ into the cell in one-to-one stoichiometry; these H^+ are then extruded (van Zweieten et al., 1981; Borregaard, Schwartz & Tauber, 1984). H^+ currents in THP-1 cells generally resembled those in other mammalian cells, but differed in their gating kinetics. In addition, both the amplitude and the kinetics of H^+ currents changed during differentiation into macrophage-like cells induced by exposure to PMA (phorbol 12-myristate 13-acetate). The final paper in the series describes changes in the expression of other ion channels in differentiated THP-1 cells (DeCoursey et al., 1996). A preliminary account of these data has been presented (DeCoursey & Cherny, 1996).

Materials and Methods

The culture of THP-1 cells and the voltage-clamp apparatus and procedures are described in Kim et al. (1996). All experiments were done at 20°C. The induction of differentiation by phorbol esters is described in DeCoursey et al. (1996).

SOLUTIONS

Most internal and external solutions were made with 100 mM buffer and 80 mM tetramethylammonium methanesulfonate ($TMAMeSO_3$) ti-

trated with tetramethylammonium hydroxide (TMAOH). A stock solution of TMAMeSO₃ was made by neutralizing TMAOH with methanesulfonic acid (Aldrich Chemical, Milwaukee, WI). Some external solutions induced 3 mM CaCl₂ and 1 mM EGTA; the pH_o 6.0 and 8.5 solutions included 1 mM EGTA and 2 mM CaCl₂. Solutions at pH 5.5, 6.5, and 7.5 included 1 mM EGTA and 2 mM MgCl₂ and were used both in the pipette and externally. No difference was observed between H⁺ currents bathed in 2 mM Ca²⁺ and 2 mM Mg²⁺. EGTA added to external solutions enhances H⁺ currents, perhaps by chelating contaminant metal ions (Cherny, Markin & DeCoursey, 1995). The pH 4.0 solution included (in mM): 150 NMG⁺ (n-methyl-D-glucamine), 50 citrate, 5 EGTA, titrated with methanesulfonic acid. Buffers (Sigma Chemical, St. Louis, MO), which were used near their pK_a, were pH 5.5–6.0 MES (2-[N-Morpholino]ethanesulfonic acid), pH 6.5 BIS-TRIS (bis[2-Hydroxyethyl]imino-tris[hydroxymethyl]methane), pH 7.0 BES (N,N-bis[2-Hydroxyethyl]-2-aminoethanesulfonic acid), pH 7.5 HEPES (N-[2-Hydroxyethyl]piperazine-N'-[2-ethanesulfonic acid]), pH 8.5 TRICINE (N-tris[Hydroxymethyl]methylglycine).

Seals were formed with Ringer's solution (160 NaCl, 4.5 KCl, 2 CaCl₂, 1 MgCl₂, 5 HEPES, pH 7.4) in the bath, and the zero current potential established after the pipette was in contact with the cell. The combined correction for the liquid junction potentials at the initial pipette/bath interface and subsequent bath/reference electrode interfaced derived from measured values amounted to 2–3 mV and was nearly identical for each combination of pipette and bath solutions used. Therefore, no junction potential correction has been applied to the data. Raw data are presented without correction for leak current. To quantitate I_H and g_H amplitudes, a usually small linear leak conductance was subtracted based on currents during subthreshold pulses. Under certain extreme conditions, when a cell became leaky or an additional time-independent and possibly nonlinear conductance was present, the H⁺ current was defined as the time-dependent component. No other time-dependent conductances were observed consistently under the ionic conditions employed.

DATA ANALYSIS

Fitting digitized currents, $I(t)$, with a single exponential was done by adjusting by eye the amplitude, A , time constant, τ , and steady-state current, I_{ss} , of a curve drawn according to: $I(t) = A(\exp(-t/\tau) + I_{ss})$, which was superimposed on the data points. When a delay was included for extracting τ_{act} values, current waveforms calculated with this equation were simply shifted in time by the amount of the delay. Differences between groups of data are evaluated by student's (two-tailed) t -test.

Results

The two main goals of this study are to describe the properties of H⁺ currents in THP-1 monocytes and to compare these properties in cells differentiated into macrophage-like cells by incubation with PMA. As the properties of H⁺ currents in THP-1 cells are described, we will mention any differences found between the two groups of cells. All illustrated data were obtained in the nominal absence of permeant ions other than H⁺ (see Materials and Methods). In the presence of "normal" ions it was still possible to observe H⁺ currents, but the data were then complicated by the superposition of the many other conductances in these cells.

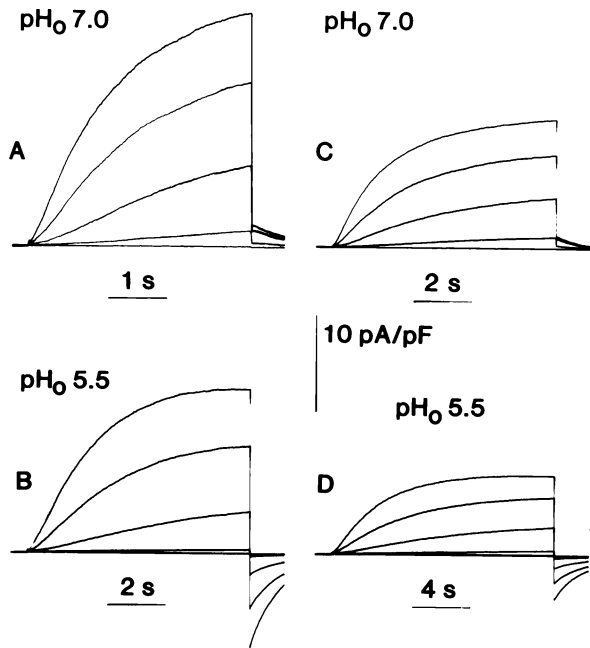


Fig. 1. Families of H⁺ currents in an undifferentiated THP-1 monocyte at pH 7.0//5.5 (A) and at pH 5.5//5.5 (B), and in a PMA-differentiated macrophage at pH 7.0//5.5 (C) and at pH 5.5//5.5 (D). Our convention is to describe the pH in the format pH_o//pH_i. In A and C currents are superimposed for pulses to -40 through +40 mV in 20 mV increments from a holding potential, $V_{hold} = -60$ mV. In B and D currents are superimposed for pulses to +20 through +100 mV in 20 mV increments from $V_{hold} = -20$ mV. Currents from both cells are scaled according to capacity, 13.4 pF (A and B) or 23 pF (C and D). Note the slower timebase at pH_o 5.5 compared with 7.0, and in the PMA-induced macrophage compared with the THP-1 monocyte. Filter 100–200 Hz.

Figure 1 illustrates families of H⁺ currents at pH_o 7.0 and pH_o 5.5 in a representative undifferentiated THP-1 monocyte (A and B), and in a PMA-differentiated macrophage (C and D), both with pH_i 5.5. As in other mammalian cells, H⁺ currents were activated slowly during depolarizing voltage pulses. The time course of the increase in H⁺ current during voltage pulses was generally sigmoidal. As is evident in Fig. 1, the H⁺ current does not reach a steady level even during quite long pulses over most of the voltage range studied. We limited the pulse duration because extremely long pulses tended to produce evidence of depletion of protonated buffer from the cell (cf. DeCoursey & Cherny, 1994a,b) and also tended to destroy the cell membrane. Lowering pH_o shifted the voltage-activation curve to more positive potentials. At pH_o 7.0 the g_H was clearly activated at -20 mV, but at pH_o 5.5 time-dependent outward H⁺ current was evident first at +40 mV. Only outward steady-state currents were observed at any pH.

The general properties of H⁺ currents were similar in THP-1 cells before and after differentiation, but several quantitative differences were observed. H⁺ currents in PMA-induced macrophages were somewhat smaller and

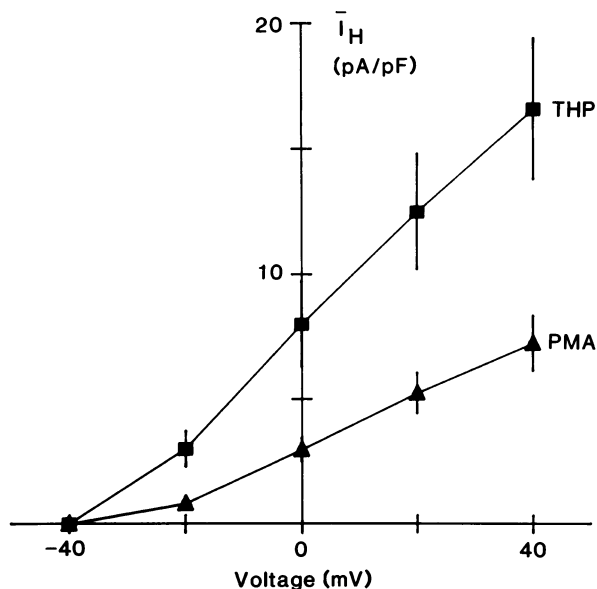


Fig. 2. Mean \pm SE \bar{I}_H at pH 7.0/5.5 in undifferentiated monocytes (THP, ■, $n = 9-10$) and PMA-differentiated macrophages (PMA, ▲, $n = 20-22$). The I_H values are the amplitude of single exponentials fitted to the H^+ currents as described in Fig. 5 and in the text. This procedure “corrects” the amplitude for leak current and for currents which did not reach steady state by the end of the pulse. Values are normalized to cell size by dividing by the capacity of each cell. All I_H values at -20 through +40 mV are significantly different ($P < 0.005$) in control vs. differentiated cells.

activated more slowly than in undifferentiated THP-1 monocytes. The average H^+ current density (normalized to cell capacity), \bar{I}_H , in the two groups at pH 7.0/5.5 is compared in Fig. 2. \bar{I}_H in differentiated cells was on average about half as large as in control THP-1 cells, but the position of the voltage-activation curve appeared to be the same. PMA-induced macrophages were larger than undifferentiated THP-1 monocytes, with average capacities of 38 ± 13 pF (mean \pm SD, $n = 22$) and 25 ± 15 pF ($n = 10$), respectively. Without correction for cell size the mean total H^+ current amplitude at +40 mV was 420 pA in undifferentiated monocytes, and 34% smaller, 277 pA, in PMA-differentiated macrophages.

Figure 3 illustrates average values for V_{rev} measured using tail currents as will be illustrated in Fig. 6. The data from both groups of cells are close to E_H , the Nernst potential for H^+ (*continuous*). The deviation of each mean value for V_{rev} from E_H was <10 mV. The slope of the linear regression line on all the data points is -55.2 mV/Unit pH. When V_{rev} was determined at both pH_o 7.0 and 5.5 in individual cells, the average difference was 84.7 ± 3.5 mV ($n = 15$, including cells before and after differentiation), very close to 87.3 mV predicted by the Nernst equation. This agreement demonstrates that the g_H is extremely selective for H^+ over TMA^+ , with a relative permeability $P_H/P_{TMA} > 10^7$, according to the Goldman-Hodgkin-Katz voltage equation. In addition,

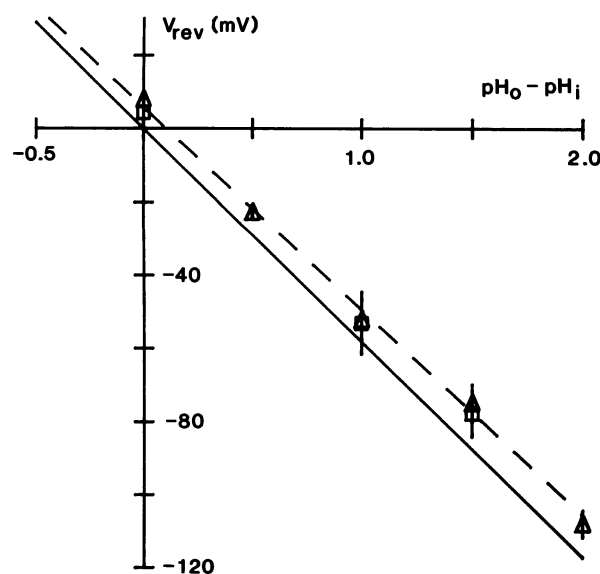


Fig. 3. Measured V_{rev} plotted against pH gradient, $pH_o - pH_i$. Mean \pm SD ($n = 3-15$) is plotted for undifferentiated THP-1 monocytes (□) and for PMA-induced macrophages (△). Of the 57 measurements included, 7 were at pH_i 6.5, and 50 were at pH_i 5.5. Solid line shows E_H calculated from the Nernst equation, and the dashed line shows the linear regression on the data points (weighted, including 3 points not plotted because $n < 3$). The slope was -55.2 mV/Unit pH.

both pH_o and pH_i must have been well controlled, because any H^+ depletion or shunt would cause a discrepancy between E_H and V_{rev} .

EFFECT OF pH_o ON H^+ CURRENTS

A hallmark feature of voltage-activated H^+ currents is their regulation by pH_o and pH_i . I_H - V relations in one cell at three pH_o are plotted in Fig. 4. The g_H was activated at -60 mV at pH_o 7.5, -20 mV at pH_o 6.5, and at +20 mV at pH_o 5.5. The I_H - V relation appears to shift to more positive potentials by 40 mV/Unit decrease in pH_o . This result is identical to that for H^+ currents in rat alveolar epithelial cells (Cherny et al., 1995). This general rule that the I_H - V relation shifted ~40 mV/Unit pH_o held for THP-1 cells both before and after differentiation.

GATING KINETICS

Inspection of Fig. 1 suggests that H^+ current activation was slower in PMA-differentiated cells. This impression is tested quantitatively in Fig. 5. The activation time course could be fitted reasonably well in most cells by a single rising exponential after a delay. Average activation time constants, τ_{act} , obtained by this procedure are plotted in Fig. 5 for two different pH_o . At more positive potentials τ_{act} decreased by about e-fold/40 mV. At each voltage at either pH_o , τ_{act} was larger in differentiated macrophages (▲) than in undifferentiated THP-1 monocytes (■), by an average of 1.9-fold. In both types of cells, lowering pH_o from 7.0 to 5.5 at constant pH_i 5.5

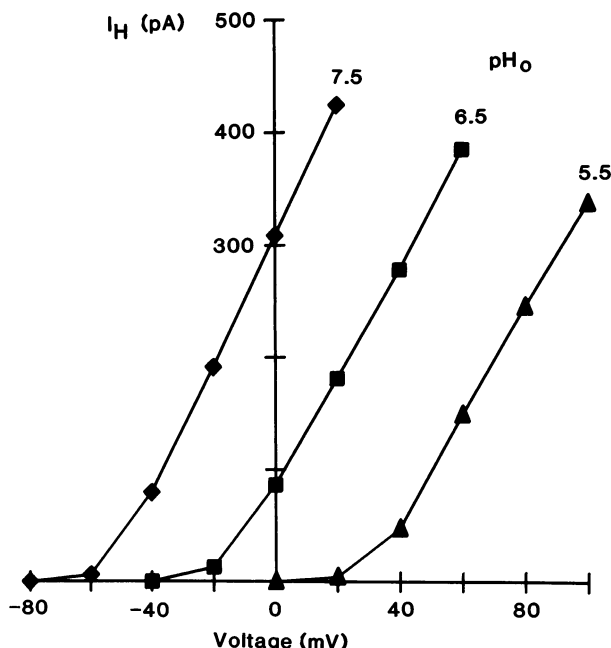


Fig. 4. Effect of pH_o on I_H - V relationships in a cell at pH_i 5.5.

shifted the $\tau_{\text{act}}-V$ relation to more positive potentials by about 90 mV. However, there appears to be a general slowing at low pH_o for a given level of activation in addition to a shift along the voltage axis, so the effect of pH_o cannot be described as a simple voltage shift.

Tail current measurements were used to determine the reversal potential, V_{rev} , the tail current time constant, τ_{tail} , and instantaneous current-voltage relations. Tail currents recorded in a PMA-differentiated cell are plotted in Fig. 6A-C at three pH_o . After a depolarizing prepulse which activated the g_H , test pulses were applied to a range of potentials. The tail current decayed completely at potentials negative to V_{rev} , and the decay was faster at more negative potentials. The decay of tail currents was well-fitted by a single exponential at all potentials. The tail current time constants, τ_{tail} , for the currents in Fig. 6A-C and also at pH_o 6.0 and 7.0 in the same cell are plotted in Fig. 6D. Over large overlapping voltage ranges, the values were identical at different pH_o . Remarkably, τ_{tail} appeared to be completely independent of pH_o . The symbols plotted at the bottom of Fig. 6D near the voltage axis show V_{rev} measured in this cell in each solution. It can be seen that τ_{tail} was the same at a given potential at different pH_o whether the tail currents were inward or outward.

CHANGES WITH TIME IN WHOLE-CELL CONFIGURATION

In each cell, τ_{tail} determined early in the experiment (15–25 min after establishing whole-cell configuration)

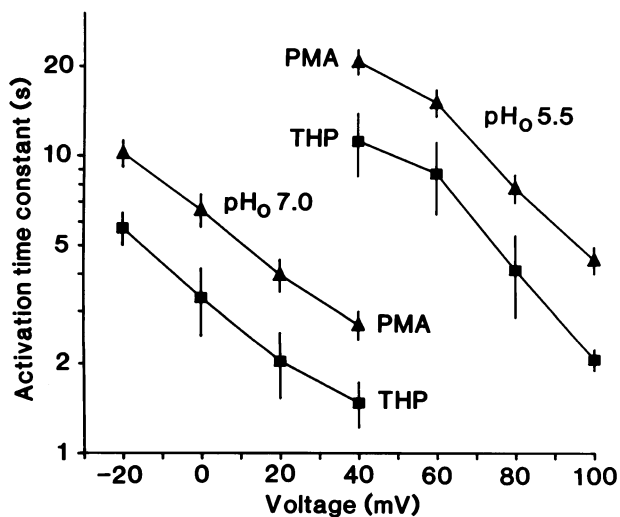


Fig. 5. Activation time constants, τ_{act} , in undifferentiated THP-1 monocytes (■) and in PMA-induced macrophages (▲), both at pH_o 7.0 and at pH_o 5.5, all with pH_i 5.5. Plotted are means \pm SEM for $n = 4$ –18 cells. All τ_{act} values are significantly faster in control cells ($P < 0.05$). See text for details.

tended to be slower by a factor of about two, than in subsequent measurements, which were quite stable over periods up to hours. We have no explanation for this phenomenon, but can rule out incomplete equilibration of buffer¹ because V_{rev} (and hence pH_i) did not change consistently during the time that τ_{tail} became faster. The τ_{tail} values plotted in Fig. 6D were all recorded after the initial equilibration period. τ_{act} also appeared to become slightly faster over the first tens of minutes in whole-cell configuration.

INSTANTANEOUS CURRENT-VOLTAGE RELATIONSHIP (I_o - V)

Although in the steady state only outward H^+ currents were seen, this rectification is not due to an inability of the open H^+ channel to conduct inward current. The prepulse in the tail current procedure opens a constant fraction of available H^+ channels, and the “instantaneous” current, I_o , measured immediately after the subsequent test pulse shows the H^+ current through these channels at the test potential. I_o - V relationships for the experiment in Fig. 6D are plotted in Fig. 6E. Over the voltage range explored, the I_o - V relationship was approximately linear at symmetrical pH 5.5/5.5, and exhibited slight outward rectification at higher pH_o . Thus H^+ channels in THP-1 cells can conduct inward and outward current equally well, and the absolute outward rectification of steady-state currents must reflect a gating mechanism which closes H^+ channels at potentials negative to E_H .

¹ but not necessarily of some other, more slowly diffusible factor

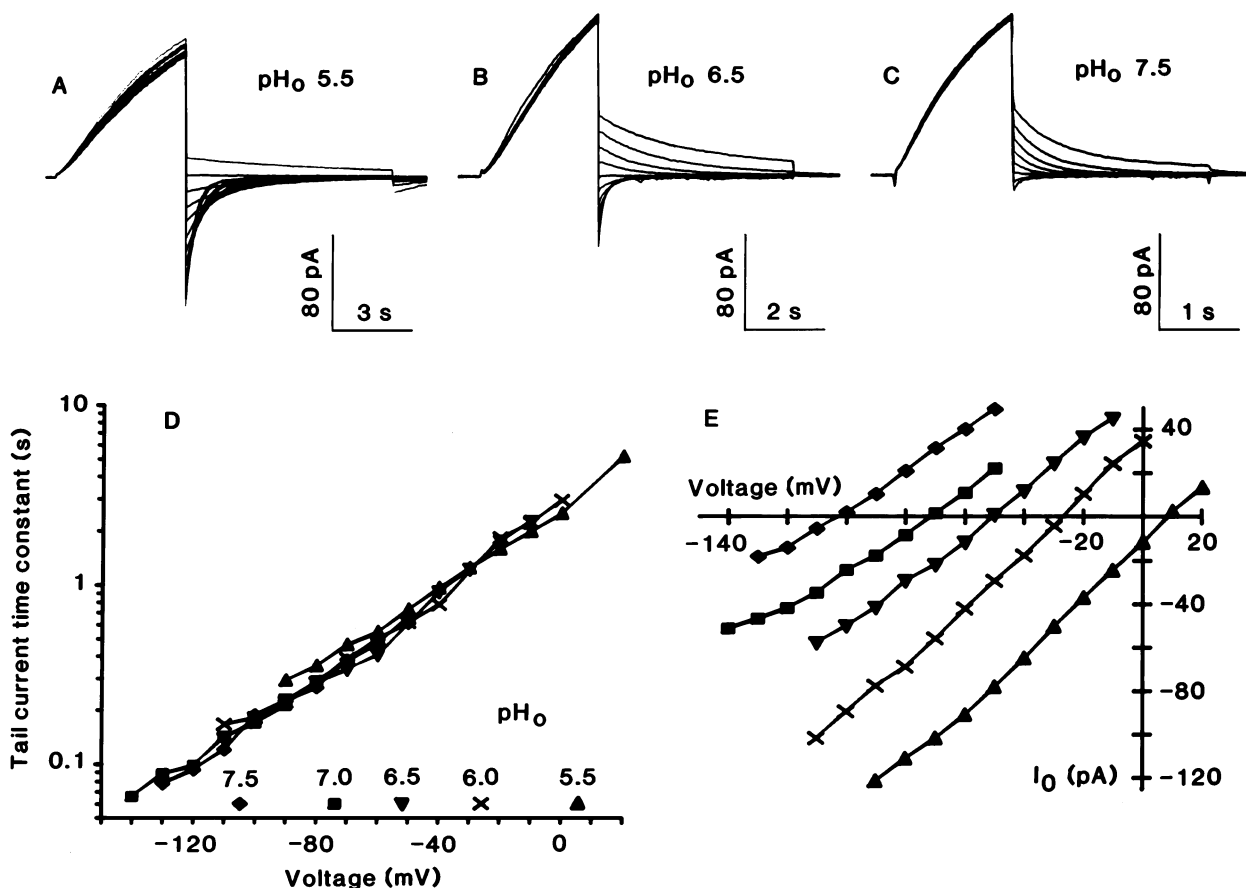


Fig. 6. Tail currents in a PMA-differentiated cell with pH_i 5.5 and pH_o 5.5 (A), 6.5 (B), or 7.5 (C). Illustrated tail currents are in 10 mV increments from -90 to +20 mV (A), -110 to -10 mV (B), and -120 to -50 mV (C). V_{hold} and the prepulse potential were -20 and +90 mV (A), -40 and +45 mV (B), and -70 and +5 mV (C). (D) Tail current time constants, τ_{tail} , from the same experiment, including also pH_o 6.0 and pH_o 7.0. Values for τ_{tail} at a given pH_o are connected by lines; symbols near the voltage axis indicate V_{rev} measured in each solution in this cell, and provide a key to symbol definition. (E) Instantaneous current-voltage relations obtained by fitting the tail current relaxation with a single exponential. The “instantaneous” current, I_0 , was defined as the amplitude of the exponential; hence the most positive point in each data set may underestimate the true I_0 because the current did not decay completely. Symbols are defined in part D.

EFFECTS OF pH_i ON H^+ CURRENTS

H^+ currents studied in cells with pH_i 6.5 (Fig. 7) or 7.5 (*not shown*), differed from those with pH_i 5.5 in two main respects. At higher pH_i (for any given pH_o) a larger depolarization was required to activate the g_{H} and the rate of H^+ current activation was slower. Insufficient data exist to compare quantitatively the voltage-activation curve at pH_i 6.5 or pH_i 7.5 with pH_i 5.5, but the results appear generally consistent with a previous systematic study in alveolar epithelial cells in which a shift of 40 mV/Unit pH_i was reported (Cherny et al., 1995). At pH_i 6.5, as illustrated in Fig. 7, changes in pH_o shifted the $I_{\text{H}}-V$ relationship by 40 mV/Unit pH_o just as described above for pH_i 5.5. Thus, H^+ current was activated at +30 mV at pH_o 6.5, at -10 mV at pH_o 7.5, and at -50 mV at pH_o 8.5. In summary, the voltage-activation curve apparently is shifted to more negative

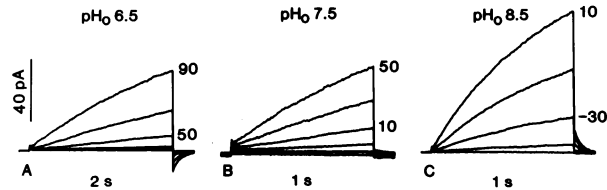


Fig. 7. Families of H^+ currents in a cell studied with pH_i 6.5 and pH_o 6.5 (A), 7.5 (B), or 8.5 (C). Currents illustrated are in 20 mV increments, as labeled. Pulse duration was 8 sec in A and 4 sec in B and C. V_{hold} was -30 mV (A), -70 mV (B), or -90 mV (C). Capacity was 10.3 pF, filter 100–200 Hz.

potentials by ~40 mV/Unit decrease in pH_i or increase in pH_o .

The H^+ currents in the cell in Fig. 7 studied at pH_i 6.5 were far from steady-state at the end of 4-sec or even 8-sec pulses. In other experiments pulses up to 16–20

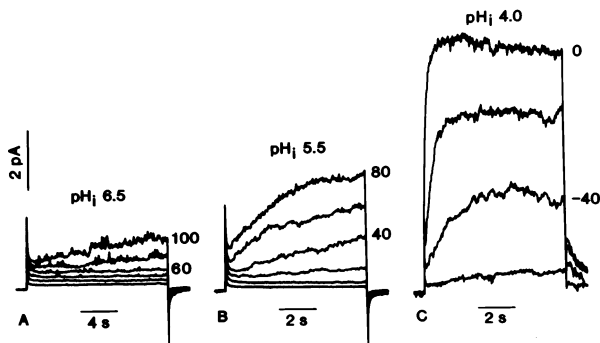


Fig. 8. H^+ currents in an inside-out patch excised from a THP-1 cell. The pipette contained pH 6.5 solution, and the bath pH 6.5 (A), 5.5 (B) or 4.0 (C) solutions. Currents are plotted in 20 mV increments, as labeled. All parts have the same current scale, but note the slower time base in A. V_{hold} was -20, -60, and -80 mV. 20 Hz filter.

sec were applied, although cells generally survived only a few extremely long pulses. The average τ_{act} at +80 mV was 8.3 ± 3.6 sec (mean \pm SD, $n = 3$) at pH 7.0//6.5. If we assume that changes in the pH gradient shift the position of the voltage-activation relationship of H^+ currents by 40 mV/Unit (Cherny et al., 1995), this value can be compared with $\tau_{act} = 1.5 \pm 0.6$ sec (mean \pm SD, $n = 6$) at +40 mV at pH 7.0//5.5., or 2.1 ± 0.3 sec ($n = 4$) at +100 mV at pH 5.5//5.5. Increasing pH_i from 5.5 to 6.5 thus slowed activation by 4–6 fold.

H^+ CURRENTS IN EXCISED PATCHES

The effects of pH_i on H^+ currents can be observed directly in excised inside-out membrane patches. Figure 8 illustrates H^+ current families in the same patch with the bath pH, corresponding with pH_i , at 6.5 (A), 5.5 (B), or 4.0 (C). The small current amplitude precludes quantitative conclusions, but the voltage-activation curve clearly shifted to more negative potentials as pH_i was decreased. H^+ currents in excised patches tended to decrease with time, especially in the first few minutes after patch excision, so the current amplitudes are of limited quantitative value. Nevertheless, it can be stated generally that lowering pH_i increased the g_H distinctly, but by far less than 10-fold per Unit pH as would be predicted if the g_H were directly proportional to the H^+ concentration, e.g., as in the Goldman-Hodgkin-Katz current equation.

An effect of pH_i on the rate of H^+ current activation is obvious in Fig. 8. At pH_i 6.5 the currents were clearly not near steady-state by the end of 16-sec pulses. Activation was faster at pH_i 5.5, and much faster at pH_i 4.0. These data are consistent with a previous study of inside-out patches of rat alveolar epithelial cells, in which intracellular protons were found to have a similarly strong effect, increasing the rate of H^+ current activation (DeCoursey & Cherny, 1995).

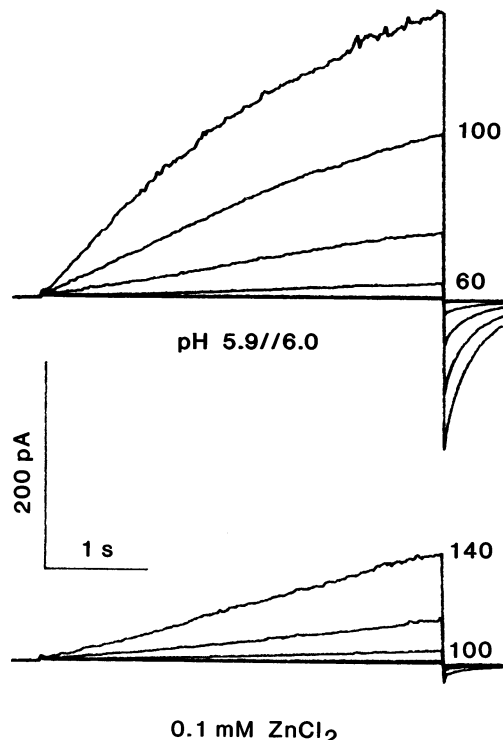


Fig. 9. Inhibition of H^+ currents by 100 μM $ZnCl_2$. From $V_{hold} = -40$ mV, 4 sec-pulses were applied in 20 mV increments, as labeled. In this experiment the external solution was TEAMESO₃ with 2 mM $CaCl_2$ and 20 mM MES buffer at pH 5.9 (without EGTA to avoid chelating the Zn^{2+}), and the pipette contained 130 mM TEAMESO₃, 20 mM MES, 5 mM EGTA, and 2 mM $MgCl_2$.

BLOCK BY DIVALENT CATIONS

All voltage-activated H^+ currents are inhibited by polyvalent metal cations (references cited in DeCoursey & Cherny, 1994a). Figure 9 confirms that H^+ currents in THP-1 cells share this property. The currents observed in the presence of 100 μM $ZnCl_2$ were greatly reduced. Block was dependent on voltage, that is to say, block was relieved by depolarization. Depolarization by ~50 mV beyond that in the absence of Zn^{2+} resulted in roughly the same current as in its absence. The effects of Zn^{2+} are consistent with its neutralizing local negative charges near H^+ channels, or electrostatically reducing the local H^+ concentration. However, a surface charge mechanism cannot account fully for the effects of divalent cations on H^+ currents (Byerly, Meech & Moody, 1984).

Discussion

COMPARISON WITH H^+ CURRENTS IN OTHER MAMMALIAN CELLS

Voltage-activated H^+ currents were present in undifferentiated THP-1 monocytes and in cells induced by PMA

to differentiate into macrophage-like cells. The g_H activated slowly during depolarizing pulses with a sigmoidal time course. The position of the voltage-activation curve depended strongly on pH, shifting 40 mV/Unit decrease in pH_o and at least that amount for increases in pH_i . Voltage-activated H^+ currents in mammalian cells generally resemble those in molluscan neurons, with the exception of their kinetics of activation. The rate of H^+ current activation during depolarizing voltage pulses is much slower in mammalian cells than in snail neurons, where H^+ currents were first described (Thomas & Meech, 1982; Byerly et al., 1984). In mammalian cells τ_{act} is in the range of seconds (DeCoursey, 1991; DeCoursey & Cherny, 1993, 1995; Bernheim et al., 1993; Kapus, Romanek & Grinstein, 1994), whereas in snail neurons half-maximal H^+ current is reached in <25 msec (Byerly et al., 1984), and in axolotl $\tau_{act} < 300$ msec (Barish & Baud, 1984). Among mammalian cells, H^+ current activation appears to be slower in THP-1 cells than in rat alveolar epithelial cells (DeCoursey, 1991; Cherny et al., 1995) or in murine macrophages (Kapus et al., 1994), and is comparable with the extremely slow activation in human neutrophils (DeCoursey & Cherny, 1993) and Chinese hamster ovary cells (Cherny, Henderson & DeCoursey, 1996). The absence of voltage-gated inward current channels, such as Na^+ or Ca^{2+} , most likely means that the membrane potential of phagocytes will not undergo rapid changes, in contrast with that of electrically excitable cells like neurons. If the g_H of phagocytes never experiences membrane depolarization in the millisecond time scale, rapid activation would serve no function. In addition, assuming that the main function of H^+ currents is to extrude cytoplasmic acid, relatively slow changes in pH_i would not require a rapidly activating g_H , but rather one which does not inactivate during sustained metabolic acid production.

Deactivation kinetics have been neglected in most previous studies of H^+ current gating. In THP-1 cells the decay of tail currents was well-fitted by a single exponential at all potentials. The time constant, τ_{tail} , was rather slow, decreasing from 2–3 sec at 0 mV to ~100 msec at -120 mV. Surprisingly, τ_{tail} was completely independent of pH_o . In rat alveolar epithelial cells, tail currents could be described by a single exponential only at potentials negative to V_{rev} , whereas at more positive potentials near the threshold for activating H^+ currents, a distinct slower component of current decay was observed (Cherny et al., 1995). The faster component was at most weakly dependent on pH_o , but the slower component was shifted by ~40 mV/Unit pH_o . Evidently, τ_{tail} in THP-1 cells reflects the equivalent of the faster component of deactivation in alveolar epithelial cells, in that both are practically independent of pH_o . The absence of a slower decay component in THP-1 cells may reflect quantitative differences in the relative rates of the several steps in channel gating, or perhaps a different mechanism alto-

gether. The insensitivity of τ_{tail} to pH_o suggests that the first step in channel closing is independent of pH_o . This interpretation is consistent with a gating model proposed recently in which deprotonation at an intracellular site or sites is the first step in channel closing (Cherny et al., 1995).

Studied in inside-out patches, the effects of changes in pH_i on H^+ currents were generally similar to those described for alveolar epithelial cells, in which lowering pH_i increased g_H by 1.7/Unit between pH 7.5 and 5.5 (DeCoursey & Cherny, 1995). Here we observed a similar pattern, but extended the range of observation to pH_i 4.0. Because the g_H increased much less than did the H^+ concentration, it seems clear that the rate-limiting step in permeation is not diffusion of H^+ to the intracellular mouth of the channel, but instead is some step during permeation itself. In a simple water-filled pore like gramicidin, the H^+ current is directly proportional to the H^+ concentration over a wide range (see DeCoursey & Cherny, 1994a); we infer that voltage-gated H^+ channels conduct protons by a different mechanism. The rate of H^+ channel activation during depolarizing pulses increased dramatically as pH_i was lowered both in inside-out patches (Fig. 8) and in macroscopic measurements, whereas changes in pH_o had much smaller effects on τ_{act} (e.g., Fig. 7). This behavior is consistent with the predominance of internal over external H^+ in setting the rate of g_H activation in alveolar epithelial cells (DeCoursey & Cherny, 1995).

FUNCTION OF H^+ CURRENTS IN PHAGOCYTES

The properties of H^+ currents in THP-1 cells closely resemble those in other phagocytes and related cell lines (reviewed by DeCoursey & Cherny, 1994a). The voltage-dependence of activation of the g_H depends on the pH gradient, ΔpH , such that increased pH_o or decreased pH_i shifts the g_H -V relationship to more negative potentials. We are aware of no studies of the resting potential or pH_i of THP-1 cells. A wide range of values (-15 to -90 mV) for the membrane potential of macrophage-related cells has been reported, in part due to technical difficulties in the measurement (Gallin & McKinney, 1990). Assuming that THP-1 cells have pH_i near 7.1 like human macrophages (Gallin & McKinney, 1990) and that pH_o is 7.4, the g_H would first be activated at a threshold potential, $V_{threshold}$, of +8 mV, according to the empirical relationship established between these parameters: $V_{threshold}$ (mV) = 20 – 40 [pH_o – pH_i] (Cherny et al., 1995). Lowering pH_i (or increasing pH_o) would shift $V_{threshold}$ to more negative values. The dependence of g_H activation on the pH gradient prevents activation at potentials negative to E_H , which would result in H^+ influx, acid-loading the cell.

The g_H of phagocytes appears to become activated during the respiratory burst, in which it helps to dissipate

intracellular H^+ generated by the electrogenic NADPH oxidase (Henderson et al., 1987, 1988a,b). Cadmium and zinc inhibit H^+ currents (see DeCoursey & Cherny, 1994a) and attenuate the respiratory burst both in human neutrophils (Henderson et al., 1988b) and in human monocytes and THP-1 cells (Leibbrandt & Koropatnick, 1994). Other pH-regulating transporters, including Na^+-H^+ antiport and $H^+-ATPase$, also likely contribute to H^+ extrusion. Na^+-H^+ antiport seems to play a major role in neutrophils, but appears to play a smaller role in macrophages (Murphy & Forman, 1993; Bidani, Brown & Heming, 1994). Of these membrane transporters, H^+ channels and the $H^+-ATPase$ are electrogenic and hence can dissipate excess positive charge in the cell resulting from the electrogenic NADPH oxidase (Henderson et al., 1987). In responding to membrane potential, the H^+ channel (but not the voltage-insensitive Na^+-H^+ antiporter) is self-limiting, and will turn itself off when the H^+ efflux has repolarized the membrane potential sufficiently. The $H^+-ATPase$ requires ATP and Na^+-H^+ antiport indirectly consumes ATP because it is driven by the Na^+ gradient, generated ultimately by the Na^+/K^+ -ATPase. In contrast, voltage-gated H^+ channels extrude H^+ at no metabolic cost to the cell, and can alkalinize the cytoplasm at a maximal rate 1–2 orders of magnitude faster than other transporters (see DeCoursey & Cherny, 1994a).

The g_H of THP-1 cells has the capacity to compensate for all of the acid produced during the respiratory burst. NADPH oxidase produces one intracellular proton per O_2^- released; two O_2^- molecules spontaneously dismutate to form H_2O_2 (Test & Weiss, 1984; Borregaard et al., 1984). Each THP-1 cell activated acutely with LPS releases $3.3 \times 10^6 H_2O_2/\text{sec}$ (Leibbrandt & Koropatnick, 1994), the equivalent of 1.0 pA of H^+ current. THP-1 cells challenged with human squamous cell carcinoma cells released $6 \times 10^5 O_2^-/\text{cell} \cdot \text{sec}$ (Takano et al., 1990), equivalent to ~90 fA of H^+ current. Because H^+ currents in THP-1 cells were 2–3 orders of magnitude larger than these values, only a small level of activation of the g_H would suffice to extrude all of the acid produced during the respiratory burst.

CHANGES IN H^+ CURRENTS WITH DIFFERENTIATION

H^+ currents were about half as large, normalized to membrane capacity, in THP-1 macrophages differentiated by PMA as in undifferentiated monocytes (Fig. 2). In addition, activation of the g_H was slower, with τ_{act} almost doubled (Fig. 5). These changes are in the opposite direction from what one might predict if the presence or amplitude of the g_H were correlated closely with the acquisition of differentiation-associated functional capabilities. Human U937 cells have a greatly enhanced capacity to produce O_2^- after differentiation (Andrew et

al., 1987; Roberts et al., 1991; Kimura, Kameoka & Ikuta, 1993). PMA-induced O_2^- production increases 10-fold in human Mono Mac 6 cells induced to differentiate by TNF (Weber et al., 1993). When HL-60 cells are induced to differentiate along the granulocytic line, I_H increases 7-fold, paralleling the appearance of NADPH oxidase and the capacity of the cells to release O_2^- and suggesting a functional association (Qu et al., 1994). However, undifferentiated THP-1 cells stimulated acutely with LPS are already capable of O_2^- production (Leibbrandt & Koropatnick, 1994) as large or larger than that measured in cultured human monocytes (Zeller et al., 1988) or rat alveolar macrophages stimulated with concanavalin A (Cameron, Nelson & Forman, 1983). A comparison of the responses of human monocytes and THP-1 cells revealed some differences, but the respiratory burst induced acutely by PMA was the same in THP-1 cells as in human monocytes (Vaddi & Newton, 1994). A contradictory study failed to detect PMA-inducible H_2O_2 release in control THP-1 cells, but observed a respiratory burst after 7 days of differentiation by retinoic acid (Mirossay et al., 1994). The apparent ability of undifferentiated THP-1 cells to secrete O_2^- may reflect that THP-1 cells are already at a more differentiated stage than other human myeloid cell lines such as HL-60 (Auwerx, 1991) or U937 (Hass et al., 1989). In addition, the combination of changes in H^+ currents in differentiated THP-1 cells may not significantly reduce the ability of the cells to extrude acid by this mechanism because the capacity for H^+ extrusion by the g_H is so large, nearly two orders of magnitude greater than that of other H^+ extruding transporters (DeCoursey & Cherny, 1994a). In other words, there is no *a priori* reason to expect that the amplitude of the g_H would be strictly correlated with the magnitude of the NADPH oxidase system. As discussed above, the g_H is large enough to extrude acid produced during the respiratory burst. However, the results seem to speak against the suggestion (Henderson & Chappell, 1992; Qu et al., 1994; Henderson, Banting & Chappell, 1995) that the H^+ channel is a component of the NADPH oxidase system.

That the kinetics of H^+ channel gating were altered during differentiation suggests that H^+ channels can be regulated by physiological mediators. The mechanism of this modulation during differentiation is an intriguing question. Perhaps properties of the g_H are sensitive to cytoplasmic second messengers. Arachidonic acid, the only known H^+ current enhancer, increases the rate of H^+ current activation, but also shifts the voltage-activation curve to more negative potentials (DeCoursey & Cherny, 1993; Kapus et al., 1994). Activation was faster in differentiated THP-1 macrophages, but no change in the voltage-activation curve was detected. In addition, the effects of exogenous arachidonic acid were at least partially reversible, and thus might not be expected to per-

sist in dialyzed cells. The observed increase in τ_{act} with decreased g_H could be explained if the mechanism of H^+ channel formation were accelerated by a higher channel density in the membrane, for example if channel formation involved the physical diffusion of protomers in the membrane whose association formed channels (cf. Cherny et al., 1995). Further study may shed light on these questions.

The authors gratefully acknowledge the technical assistance of Donald R. Anderson. The authors appreciate constructive suggestions from one of the referees on the teleological utility of H^+ currents. This project was supported by a Grant-in-Aid from the American Heart Association and National Institutes of Health grant R01-HL52671 (TD).

References

Andrew, P.W., Robertson, A.K., Lowrie, D.B., Cross, A.R., Jones, O.T.G. 1987. Induction of synthesis of components of the hydrogen peroxide-generating oxidase during activation of the human monocytic cell line U937 by interferon- γ . *Biochem J.* **248**:281–283

Auwerx, J. 1991. The human leukemia cell line, THP-1: a multifaceted model for the study of monocyte-macrophage differentiation. *Experientia* **47**:22–31

Barish, M.E., Baud, C. 1984. A voltage-gated hydrogen ion current in the oocyte membrane of the axolotl, *Ambystoma*. *J. Physiol.* **352**:243–263

Bernheim, L., Krause, R.M., Baroffio, A., Hamann, M., Kaelin, A., Bader, C.-R. 1993. A voltage-dependent proton current in cultured human skeletal muscle myotubes. *J. Physiol.* **470**:313–333

Bidani, A., Brown, S.E.S., Heming, T.A. 1994. pH regulation in alveolar macrophages: relative roles of Na^+-H^+ antiport and H^+ -ATPase. *Am. J. Physiol.* **259**:C586–C598

Borregaard, N., Schwartz, J.H., Tauber, A.I. 1984. Proton secretion by stimulated neutrophils: significance of hexose monophosphate shunt activity as source of electrons and protons for the respiratory burst. *J. Clin. Invest.* **74**:455–459

Byerly, L., Meech, R., Moody, W. 1984. Rapidly activating hydrogen ion currents in perfused neurones of the snail, *Lymnaea stagnalis*. *J. Physiol.* **351**:199–216

Cameron, A.R., Nelson, J., Forman, H.J. 1983. Depolarization and increased conductance precede superoxide release by concanavalin A-stimulated rat alveolar macrophages. *Proc. Natl. Acad. Sci. USA* **80**:3726–3728

Cherny, V.V., Henderson, L.M., DeCoursey, T.E. 1996. Proton and chloride currents in Chinese hamster ovary cells. *Biophys. J.* **70**:A77 (Abstr.)

Cherny, V.V., Markin, V.S., DeCoursey, T.E. 1995. The voltage-activated hydrogen ion conductance in rat alveolar epithelial cells is determined by the pH gradient. *J. Gen. Physiol.* **105**:861–896

DeCoursey, T.E. 1991. Hydrogen ion currents in rat alveolar epithelial cells. *Biophys. J.* **60**:1243–1253

DeCoursey, T.E., Cherny, V.V. 1993. Potential, pH, and arachidonate gate hydrogen ion currents in human neutrophils. *Biophys. J.* **65**:1590–1598

DeCoursey, T.E., Cherny, V.V. 1994a. Voltage-activated hydrogen ion currents. *J. Membrane Biol.* **141**:203–223

DeCoursey, T.E., Cherny, V.V. 1994b. Na^+-H^+ antiport detected through hydrogen ion currents in rat alveolar epithelial cells and human neutrophils. *J. Gen. Physiol.* **103**:755–785

DeCoursey, T.E., Cherny, V.V. 1995. Voltage-activated proton currents in membrane patches of rat alveolar epithelial cells. *J. Physiol.* **489**:299–307

DeCoursey, T.E., Cherny, V.V. 1996. Voltage-activated proton currents in human THP-1 monocytes. *Biophys. J.* **70**:A415. (Abstr.)

DeCoursey, T.E., Kim, S.Y., Silver, M.R., Quandt, F.N. 1996. Ion channel expression in PMA-differentiated human THP-1 macrophages. *J. Membrane Biol.* **152**:2

Gallin, E.K., McKinney, L.C. 1990. Monovalent ion transport and membrane potential changes during activation in phagocytic leukocytes. *Curr. Top. Membr. Transp.* **35**:127–152

Hass, R., Bartels, H., Topley, N., Hadam, M., Köhler, L., Goppelt-Strübe, M., Resch, K. 1989. TPA-induced differentiation and adhesion of U937 cells: changes in ultrastructure, cytoskeletal organization and expression of cell surface antigens. *Eur. J. Cell. Biol.* **48**:282–293

Henderson, L.M., Banting, G., Chappell, J.B. 1995. The arachidonate-activatable, NADPH oxidase-associated H^+ channel. *J. Biol. Chem.* **270**:5909–5916

Henderson, L.M., Chappell, J.B. 1992. The NADPH-oxidase-associated H^+ channel is opened by arachidonate. *Biochem. J.* **283**:171–175

Henderson, L.M., Chappell, J.B., Jones, O.T.G. 1987. The superoxide-generating NADPH oxidase of human neutrophils is electrogenic and associated with an H^+ channel. *Biochem. J.* **246**:325–329

Henderson, L.M., Chappell, J.B., Jones, O.T.G. 1988a. Internal pH changes associated with the activity of NADPH oxidase of human neutrophils: further evidence for the presence of an H^+ conducting channel. *Biochem. J.* **251**:563–567

Henderson, L.M., Chappell, J.B., Jones, O.T.G. 1988b. Superoxide generation by the electrogenic NADPH oxidase of human neutrophils is limited by the movement of a compensating charge. *Biochem. J.* **255**:285–290

Kapus, A., Romanek, R., Grinstein, S. 1994. Arachidonic acid stimulates the plasma membrane H^+ conductance of macrophages. *J. Biol. Chem.* **269**:4736–4745

Kim, S.Y., Silver, M.R., DeCoursey, T.E. 1996. Ion channels in human THP-1 monocytes. *J. Membrane Biol.* **152**:2

Kimura, T., Kameoka, M., Ikuta, K. 1993. Amplification of superoxide anion generation in phagocytic cells by HIV-1 infection. *FEBS Lett.* **326**:232–236

Leibbrandt, M.E.J., Koropatnick, J. 1994. Activation of human monocytes with lipopolysaccharide induces metallothionein expression and is diminished by zinc. *Toxicol. Appl. Pharmacol.* **124**:72–81

Mirossay, L., Chastre, E., Callebert, J., Launay, J.-M., Housset, B., Zimber, A., Abita, J.P., Gespach, C. 1994. Histamine H₂ receptors and histidine decarboxylase in normal and leukemic human monocytes and macrophages. *Am. J. Physiol.* **267**:R602–R611

Murphy, J.K., Forman, H.J. 1993. Effects of sodium and proton pump activity on respiratory burst and pH regulation of rat alveolar macrophages. *Am. J. Physiol.* **264**:L523–L532

Qu, A.Y., Nanda, A., Curnutte, J.T., Grinstein, S. 1994. Development of a H^+ -selective conductance during granulocytic differentiation of HL-60 cells. *Am. J. Physiol.* **266**:C1263–C1270

Roberts, P.J., Devalia, V., Faint, R., Pizzey, A., Bainton, A.L., Thomas, N.S.B., Pilkington, G.R., Linch, D.C. 1991. Differentiation-linked activation of the respiratory burst in a monocytic cell line (U937) via Fc γ RII: a study of activation pathways and their regulation. *J. Immunol.* **147**:3104–3115

Takano, R., Nose, M., Kanno, H., Nishihira, T., Hiraizumi, S., Kobata, A., Kyogoku, M. 1990. Recognition of N-glycosidic carbohydrates on esophageal carcinoma cells by macrophage cell line THP-1. *Am. J. Pathol.* **137**:393–401

Test, S.T., Weiss, S.J. 1984. Quantitative and temporal characterization

of the extracellular H_2O_2 pool generated by human neutrophils. *J. Biol. Chem.* **259**:399–405

Thomas, R.C., Meech, R.W. 1982. Hydrogen ion currents and intracellular pH in depolarized voltage-clamped snail neurones. *Nature* **299**:826–828

Vaddi, K., Newton, R.C. 1994. Comparison of biological responses of human monocytes and THP-1 cells to chemokines of the intercrine- β -family. *J. Leukocyte Biol.* **55**:756–762

van Zweiten, R., Wever, R., Hamers, M.N., Weening, R.S., Roos, D. 1981. Extracellular proton release by stimulated neutrophils. *J. Clin. Invest.* **68**:310–313

Weber, C., Aepfelbacher, M., Haag, H., Löms Ziegler-Heitbrock, H.W., Weber, P.C. 1993. Tumor necrosis factor induces enhanced responses to platelet-activating factor and differentiation in human monocytic Mono Mac 6 cells. *Eur. J. Immunol.* **23**:852–859

Zeller, J.M., Caliendo, J., Lint, T.F., Nelson, D.J. 1988. Changes in respiratory burst activity during human monocyte differentiation in suspension culture. *Inflammation* **12**:585–595